A Bond Graph Approach to Modeling an Aeroelastic Behaviour of Wing Section in Pitch and Plunge Motion

João Bosco Martinolli
Instituto de Fomento e Coordenação Industrial - IFI
CTA – Praça Mal Eduardo Gomes N° 50
São José dos Campos – SP
Cep.: 12 228-901
e-mail joao.bosco@ifi.cta.br

Roberto Gil Annes da Silva
Instituto de Aeronáutica e Espaço - IAE
CTA – Praça Mal Eduardo Gomes N° 50
São José dos Campos – SP
Cep.: 12 228-901
e-mail: rasilva@iae.cta.br

Luiz Carlos Sandoval Góes
Instituto Tecnológico de Aeronáutica
Divisão de Engenharia Mecânica
CTA – Praça Mal Eduardo Gomes N° 50
São José dos Campos – SP
Cep.: 12 228-900
e-mail: goes@ita.cta.br

Abstract - In this paper, the linear and nonlinear aeroelastic response is modeled using bond graph with a unique experiment that allows prescribed plunge and wings pitch motion. In the first case, the equations of the mechanism of aerodynamic instability is derived using the bond-graph modeling, the lagrangian approach, the general theory of aerodynamic instability and the flutter mechanism (classical unsteady theory).

The transfer function of the linear system will be studied in different aeroelastic parameters such as freestream velocity, atmosephere density and airfoil characteristics (geometry). Incorporated with a full-state feedback control law, an optimal observer is used to stabilize the system. The simulated models are compatible with results found in available literature and control is achieved when system is undergoing limit cycle oscilattions.

Keywords: bond graph, flutter, aeroelasticity, modeling, control systems

1. NOMENCLATURE

The nomenclature used in this paper is presented on Table 1.

Table 1. Nomenclature

A, B	system matrices	a	nondimensionalized distance from the midchord to the elastic axis
α	pitch angle	β	flap deflection
b	semi-chord of the wing	c_h	structural damping coefficient in plunge due viscous damping
c_α	structural damping coefficient in pitch due viscous damping	$c_{l\alpha},c_{m\alpha}$	lift and pitch moment coefficient per angle of attack
$c_{l\beta},c_{m\beta}$	lift and pitch moment coefficient per control surface deflection	I_α	mass moment of inertia of the wing about the elastic axis
J	performance index	K_h	structural spring constant in plunge
K_α	structural spring constant in pitch	L,M	aerodynamic force and moment
m	mass	P(x)	positive definite symmetric matrix
ρ	air density	Q,R	weighting matrices
S_p	wing span	U	free stream velocity
x	states of the aeroelastic system	s_α	nondimensionalized distance measured from the elastic axis to center of mass
k	$b\omega/U$ (reduced frequency)		

2. INTRODUCTION

Aeroelasticity is the phenomena (O'Neil et al. 1998) resulting from the interaction of structural, inertial and aerodynamics forces. The aerodynamic loads on aircraft wing vary with the speed of flow and depend on the structural response.

Usually, the unsteady aerodynamic loads are divided into two parts, lift and drag, when the aerodynamic and structural loads are in balance, it will produce a harmonic oscillation. This kind of vibration happens at certain speed of flow called the flutter boundary. A literature review (Block et al. 1997) gives several examples of flutter analysis and control, as well as nonlinear aeroelastic analysis.

Theodorsen (1935) was an original investigator of flutter phenomenon. He developed an unsteady aerodynamic model that led to the popular Theodorsen´s Function. The functions explain the lag effects of the unsteady aerodynamics at different values of reduced frequency, k. Theodorsen and Garrick (1940) used this method to compare theoretical predictions of flutter velocity and frequency with experimental results. The method assumes oscillatory motion of the wing and provides an excellent means for predicting the flutter velocity and frequency. In "Introduction to the Theory of Aeroelasticity" Fung (1955) shows approximated Theodorsen´s function to simulate a wing in unsteady aerodynamic flow. With these approximations, the motion equations can be integrated and solved to show a two or three dimensional wings response. Conventional methods of examining aeroelastic behavior have relied on a linear approximation of the governing equations of the flow field and/or the structure: however, aerospace systems inherently contain structural and aerodynamic nonlinearities result from unsteady aerodynamic sources, large strain-displacement conditions, and partial loss of structural or control integrity. These systems may exhibit nonlinear dynamic response characteristics such as limit cycle oscillations, internal resonances and chaotic motion.

Flutter analysis is generally executed by mathematical modeling based on Lagrange equation and completed by solving the complex determinant of the equation in frequency domain. In it, the analysis of the problem is modeled and analyzed using power bond graph method. In this method, the phenomenon is considered as a dynamic system that consists of interacting sub-systems and/or components. All the elements within the system are connected each other by energy bonding where the power flows through. The types of the basic elements that construct the system are: the storing/dissipating energy components, energy transmitters, and junctions, beside the source of energy as the external excitations.

The contribution of this paper lies in the use of a bond graph approach to modeling an aeroelastic system (wing section) in pitch and plunge motion. In the first case, a nonlinear aeroelastic model is represented as shown by Sahjendra and Strganac, the model represents a typical aeroelastic wing section which has been traditionally used for the theoretical and experimental study of two dimensional aeroelastic behavior. In the second case, a single trailing edge control surface is used for the nonlinear aeroelastic system control. The control system design is based on the state-dependent Riccati method. This approach has been developed in a series of papers (De Marchi, Singh, Planitis and Block, 2005a, 2002b, 2004c, 1997d) and applied to variety of aerospace control problems.

3. BOND-GRAPH OF AN AEROELASTIC SYSTEM

Bond graph modeling is a powerful tool for modeling engineering systems; especially when different physical domains are involved. Furthermore, bond graph sub-models can be re-used elegantly (Broenink, 1999), because bond graph models are non-causal. Bond graphs are labeled and directed graphs, in which the vertices represent sub models and the edges represent an ideal energy connection between power ports. The vertices are idealized descriptions of physical phenomena: they are concepts, denoting the relevant aspects of the dynamic behaviour of the systems. It can be bond graphs itself, thus allowing hierarquical models, or it can be a set of equations in the variables of the ports (two at each port). The edges are called bonds.

The concept of bond graphs was originated by Paynter (1961). The idea was further developed by Karnopp et al. in their textbooks (1968, 1975, 1983, 1990), so that it could be used in practice. Damic et al. in "A Bond Graph Approach to Modeling of Spatial Flexible Multibody Systems Based on Co-rotational Formulation", developed a model to explore the application of bond graph techniques to modeling multibody systems consisting of interconnected slender bodies that undergo large translational and/or rotational motions. The results of that work are in agreement with those reported in literature, demonstrating that bond graph model is capable of capturing nonlinear phenomena that may characterize such problems. Pagwiwoko et al. (2001) examined an aeroelastic behavior using bond graph approach; the authors consider the flutter phenomena as a dynamic system constructed in the form of power bond graph, converting the bond graph model into equivalent block diagram, the analysis of structural response can be carried out directly in time domain.

Bond graphs are a domain-independent graphical description of dynamic behaviour of physical systems. This means that systems from different domains are described in the same way. The basis is that bond graphs are based on energy and energy exchange. Behaviour with respect to energy is domain independent. It is the same in all engineering disciplines, as can be concluded when comparing electrical system with the damped mass spring system. This leads to identical bond graphs.

Two elements in bond graph are connected by a bond, this bond can be interpreted in two different ways, as an interaction of energy or as a bilateral signal flow, this is essential in bond graph modeling. Modeling is started by indicating the physical structure of the system. The process of determining the computational direction of the bond variables is called causal analysis. The result indicated in the graph by so-called causal stroke, indicating the direction of the effort, and is called the causality of the bond.

The nature of the constitutive equations laid demands on the causality of the connected bonds. Bond graphs elements are drawn as letter combinations indicating the type of element. The bond graph elements are the following:

C - Storage element, capacitor, spring, store all kinds of free energy;

I - Storage element, inductor, mass;

R - Resistor dissipating free energy, electric resistor, mechanical friction;

Se/Sf - Sources, electric mains, gravity, pump, in this case represented by **Lift** and **Moment;**

0/1 - Junctions, for ideal connecting two or more submodels.

By definition, the power is positive in the direction of the power bond (direction of the half arrow). A port that has an incoming bond connected to, consumes power if this power is positive. In other words; the power flows in the direction of the half arrow if it is positive and the other way if it is negative.

To generate a bond graph model starting from an ideal-physical model, a systematic method exist, this method consists roughly of the identification of the domains and basic elements, the generation of the connected structure, the placement of the elements, and possibly simplifying the graph.

A causal bond graph contains all information to derive the set of state equations. It is either a set of ordinary first-order differential equations, when the model is explicit, or a set of differential and algebraic equations, when the model is implicit.

The aeroelastic wing section used for analysis is shown in figure 1 and the bond graph model of system is shown in figure 2.
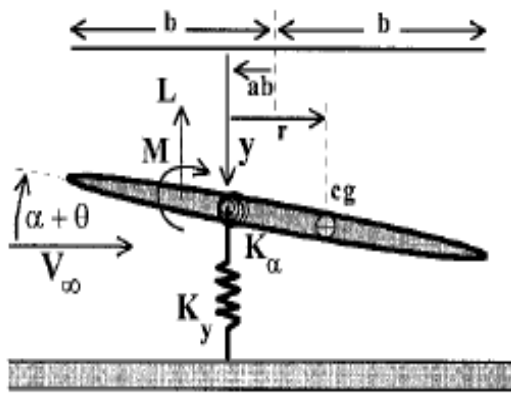
Figure 1: Aeroelastic Wing Model (O'Neill et al)
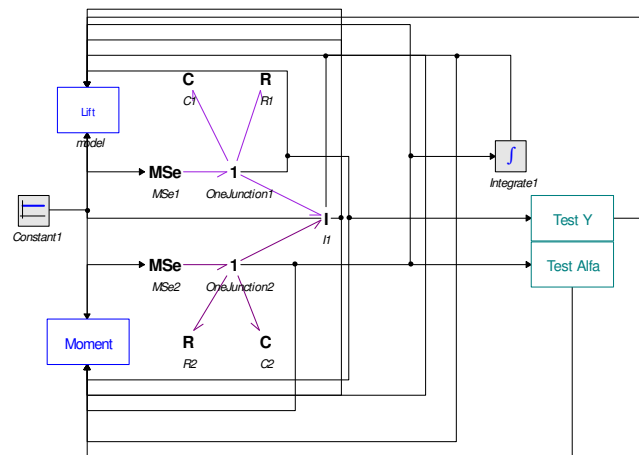
Figure 2: Bond-Graph Model of an Aeroelastic Wing

The equations associated to the model are (O'Neill et al):

$$m_T \ddot{y} + m_w r \cos(\alpha + \theta)\ddot{\alpha} - m_w r \sin(\alpha + \theta)\dot{\alpha}^2 + C_y \dot{y} + \mu_y g m_T (|\dot{y}|/\dot{y}) + k_y (y + \xi y^3) = -L$$

$$m_w r \cos(\alpha + \theta)\ddot{y} + I_e \ddot{\alpha} + C_\alpha \dot{\alpha} + \mu_\alpha g m r_b (|\dot{\alpha}|/\dot{\alpha}) + k_\alpha (\alpha + \zeta \alpha^3) = M$$

(1)

The nomenclature used in Figure 2 is presented on Table 2.

Table 2. Nomenclature used in Figure 2

C1	Stiffness Coefficient in Plunge Motion	R1	Damping Coefficient in Plunge Motion
C2	Stiffness Coefficient in Pitch Motion	R2	Damping Coefficient in Pitch Motion
One Junction 1	Plunge Velocity $\dot{y}$	One Junction 2	Pitch Velocity $\dot{\alpha}$
Constant 1	Free Stream Velocity	Lift	Block to Calculate Lift
Moment	Block to Calculate Moment	I	Inertia Element of the System
Mse 1	Modulated Source Element (for Lift)	Mse 2	Modulated Source Element (for Moment)
Test Y	$|\dot{y}|/\dot{y}$	Test Alfa	$|\dot{\alpha}|/\dot{\alpha}$

In equations (1) m_T denotes the total system mass that translates; m_w denotes the wing mass that rotates; and $I_e = r^2 m_w + I_{cg}$. Both viscous and Coulomb-type dampings are included according to the viscous damping forces, and μ_α and μ_y terms are included according to the Coulomb damping forces. Nonlinear stiffness characteristics for pitch and plunge motion are represented by the parameters ζ and ξ. It is important to note that the unsteady aerodynamic loads are dependent upon the motion of the wing, thus,

$$L = L(\dot{y}, \ddot{y}, \dot{\alpha}, \ddot{\alpha}, V_\infty, \rho, time)$$

$$M = M(\dot{y}, \ddot{y}, \dot{\alpha}, \ddot{\alpha}, V_\infty, \rho, time)$$

(2)

The aerodynamic and pitch moment are modeled by the unsteady aerodynamic theory of Theodore Theodorsen (O'Neill et al):

$$L = \pi\rho b^2 (\ddot{y} + V_\infty \dot{\alpha} - ba\ddot{\alpha}) + 2\pi\rho V_\infty Cb(\dot{y} + V_\infty \alpha + b(1/2-a)\dot{\alpha})$$

$$M = -\pi\rho b^3 [-a\ddot{y} + (1/2-a)V_\infty \dot{\alpha} + (1/8-a^2)b\ddot{\alpha}] + 2\pi\rho V_\infty Cb^2 (1/2+a)[\dot{y} + V_\infty \alpha + b(1/2-a)\dot{\alpha}]$$

(3)

In (3) C is Theodorsen´s function that depends on the reduced frequency, k = bω/V. It is noted that equation (3) represents incompressible small disturbance unsteady flow. Physical properties of the experiment hardware and associated analyses are provided next: $a = -0.450$, $m_T = 10.3kg$, $m_w = 1.662kg$, $b = 0.1064$, $s = 0.6m$, $k_\alpha = 2.57(1+1.33\alpha^2)N-m/rad$, $k_y = 2860(1+0.09y^2)N-m/rad$, $r = 0.0287m$, $C_y = 7.30kg/s$, $C_\alpha = 0.008Kg-m^2/s$, $\mu_y = 0.0125$, $\mu_\alpha = 0.0252$, $I_e = 0.0160 + r^2 m_w = 0.0174kg-m^2$, $y_0 = 0.0254m$, $\alpha_0 = 0.175rad$, $\dot{\alpha}_0 = \dot{y}_0 = 0$.

The bond-graph model for the system derived from (1-3) is shown in the Fig. 2. The Theodorsen´s function, C(k), contained within the description of the unsteady aerodynamic loads, depends on the reduced frequency k, Similar to the efforts of O´Neil et al. (1998), the impact of the assumptions contained in quasi-steady and unsteady aerodynamic models were considered. For the low reduced frequency motion of the experiments discussed herein (k ≈0.1), a quasisteady assumption is proven valid by preliminary experiments and, consequently, C(k) is set unity in this point.

4. THE BOND-GRAPH SIMULATION

The software used for the simulation of the aeroelastic model is the 20-sim, version 3.2, this software permits through appropriate symbols to create elements and connections among these to represent the associated physical model. The free stream velocity can be chosen the value of "Constant 1".

The variables $\dot{y}$ and $\dot{\alpha}$ are used for the feedback of the Lift and Pitch Moment, the system is self-excited.

Figures 3 and 4 shows the plunge and pitch motion, for simulation using V = 15 m/s, ξ =0.09 and ζ = 80.0.

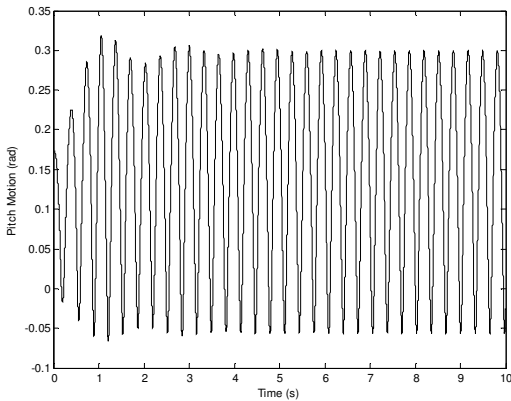Figures 5 and 6 shows the pitch and plunge motion for the same velocity and ξ =0.0 and ζ = 0.0.

Figure 3: Pitch Motion
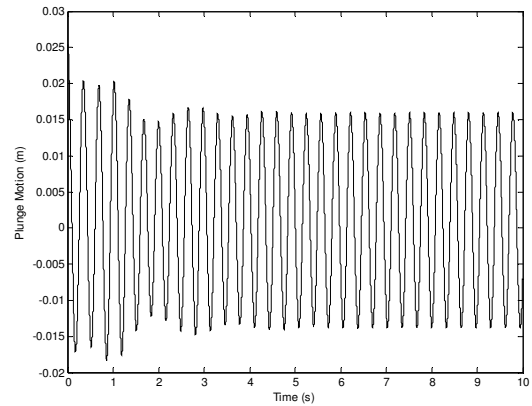for V = 15.0 m/s, ξ =0.09 and ζ = 80.0.

Figure 4: Plunge Motion
for V = 15.0 m/s, ξ =0.09 and ζ = 80.0.

5. CLOSED-LOOP MODEL SIMULATION

5.1 AEROELASTIC LINEAR MODEL

For the closed-loop model, the aeroelastic wing section is shown in fig. 7.

The bond graph model using 20-sim it is shown in fig. 8, the definitions of the model are: MSE = Modulated Source Element (vector), I – Inertia Matrix Element, R – Damping Matrix Element, C – Stiffness Matrix Element, Constant 1 – Velocity Vector $\{\dot{h}, \dot{\alpha}\}$, Constant 2 – β and Constant 3 – "a". In the first case a simulation performance in open-loop model with initial conditions; h_0= 0.02m, α_0 = 0.2 rad, $\dot{\alpha} = 0.0$ and $\dot{h} = 0.0$.
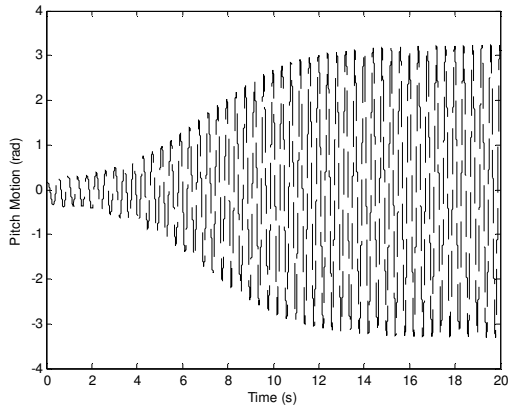
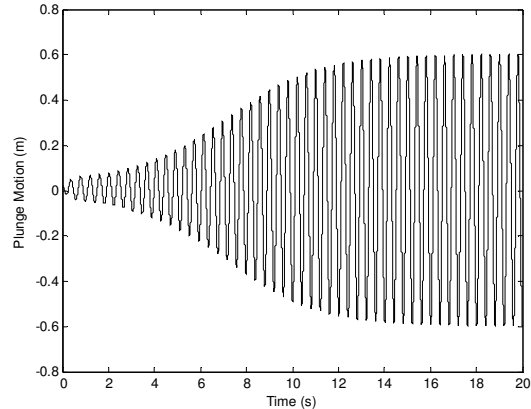Figure 5: Pitch Motion for V = 15.0 m/s, ξ =0.0 and ζ = 0.0.

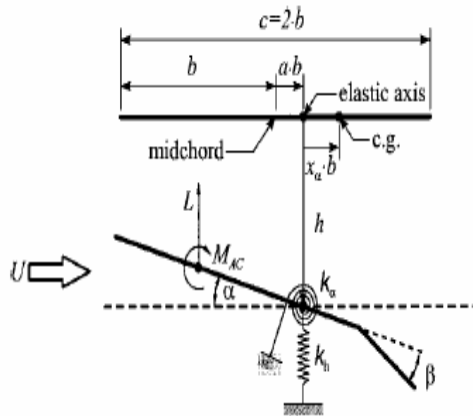Figure 6: Plunge Motion for V = 15.0 m/s, ξ =0.0 and ζ = 0.0.

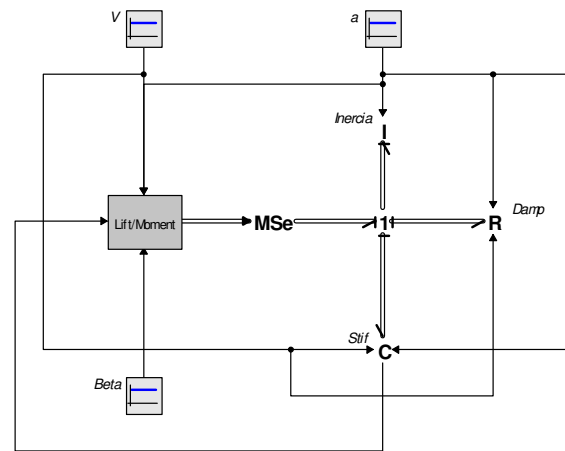Figure 7. Wing Model with Control Surface (Strganac et al)

Figure 8. Bond-Graph Model of System in Figure 7

The governing equations of motion are (Bismarck, 1997):

$$
\begin{bmatrix} m & mx_\alpha b \\ mx_\alpha b & I_\alpha \end{bmatrix} \begin{Bmatrix} \ddot{h} \\ \ddot{\alpha} \end{Bmatrix} + \begin{bmatrix} c_h & 0 \\ 0 & c_\alpha \end{bmatrix} \begin{Bmatrix} \dot{h} \\ \dot{\alpha} \end{Bmatrix} + \begin{bmatrix} k_h & 0 \\ 0 & k_\alpha \end{bmatrix} \begin{Bmatrix} h \\ \alpha \end{Bmatrix} = \begin{Bmatrix} -L \\ M \end{Bmatrix} \tag{4}
$$

M and L are the aerodynamic lift and pitch moment. It is assumed that quasi-steady aerodynamic force and moment are the forms:

$$
L = \rho U^2 s_p b c_{l\alpha} \left[\alpha + \frac{\dot{h}}{U} + \left(\frac{1}{2} - a \right) b \frac{\dot{\alpha}}{U} \right] + \rho U^2 s_p b c_{l\beta} \beta \tag{5}
$$

$$
M = \rho U^2 s_p b^2 c_{m\alpha} \left[\alpha + \frac{\dot{h}}{U} + \left(\frac{1}{2} - a \right) b \frac{\dot{\alpha}}{U} \right] + \rho U^2 s_p b^2 c_{m\beta} \beta \tag{6}
$$

where "a" is the nondimensionalized distance from the midchord to elastic axis, s_p is the wing span, $c_{l\alpha}$ and $c_{m\alpha}$ are the lift and pitch moment coefficients per angle of attack, and $c_{l\beta}$ and $c_{m\beta}$ are the lift and pitch moment coefficients per control surface deflection β. The model has a diagonal damping matrix, however it should be noted that the method is applicable to models of larger dimensions, which have nonlinear damping matrices with nonzero off-diagonal elements.

Defining the state vector $x = \{h, \alpha, \dot{h}, \dot{\alpha}\} \in$ R4, one obtains a state variable representation of (4-5-6) in the form:

$$
\dot{x} = \begin{bmatrix} 0_{2x2} & I_{2x2} \\ M_1 & M_2 \end{bmatrix} \{x\} + \begin{bmatrix} 0_{2x1} \\ b_0 \end{bmatrix} \beta \tag{7}
$$

where $b_0 = [b_{01}, b_{02}]^T$, 0_{ixj} and I_{ixj} denote null and identity matrices of appropriate dimensions.
M_1, M_2, M_3 and M_4 are like in Singh:

$$M_1 = -\begin{bmatrix} \dfrac{I_\alpha k_h}{m(I_\alpha - b^2 m^2 x^2{}_\alpha)} & \dfrac{bU^2 \rho C_{l\alpha} I_\alpha s_p - bm(k_\alpha - b^2 U^2 \rho C_{m\alpha} s_p)x_\alpha}{m(I_\alpha - b^2 m^2 x^2{}_\alpha)} \\ \dfrac{-bmk_h x_\alpha}{-(I_\alpha - b^2 m^2 x^2{}_\alpha)} & \dfrac{m(k_\alpha - b^2 U^2 \rho C_{m\alpha} sp) - b^2 mU^2 \rho C_{l\alpha} s_p x_\alpha}{(I_\alpha - b^2 m^2 x^2{}_\alpha)} \end{bmatrix} \tag{8}$$

$$M_2 = -\begin{bmatrix} \dfrac{c_h I_\alpha + bU\rho s_p(C_{l\alpha} + I_\alpha + b^2 m C_{m\alpha} x_\alpha)}{m(I_\alpha - b^2 m x^2{}_\alpha)} & \dfrac{b[2mc_\alpha x_\alpha + (-1+2a)bU\rho s_p(C_{l\alpha} I_\alpha + b^2 m C_{m\alpha} x_\alpha)]}{2m(I_\alpha - b^2 m x^2{}_\alpha)} \\ \dfrac{b[c_h x_\alpha + bU\rho s_p(C_{m\alpha} + C_{l\alpha} x_\alpha)]}{-(I_\alpha - b^2 m x^2{}_\alpha)} & \dfrac{2c_\alpha + (-1+2a)b^3 U\rho s_p(C_{m\alpha} + C_{l\alpha} x_\alpha)}{2(I_\alpha - b^2 m x^2{}_\alpha)} \end{bmatrix} \tag{9}$$

$$b_0 = \begin{bmatrix} \dfrac{bU^2 \rho s_p(C_{l\beta} I_\alpha + b^2 m C_{m\beta} x_\alpha)}{m(-I_\alpha + b^2 m x^2{}_\alpha)} \\ -\dfrac{b^2 U^2 \rho s_p(C_{m\beta} + C_{l\beta} x_\alpha)}{-I_\alpha + b^2 m x^2{}_\alpha} \end{bmatrix} \tag{10}$$

The systems parameters are: $b = 0.135m$; $c_\alpha = 0.036 Ns$, $c_{l\beta} = 3.358$, $m = 3.358$ kg, $s_p = 0.6m$, $k_h = 2844.4 N/m$, $\rho = 1.225 kg/m^3$, $c_{m\alpha} = (0.5+a)c_{l\alpha}$, $I_\alpha = 0.065 kgm^2$, $k_\alpha = 2.82 Nm/rad$, $c_h = 27.43 Ns/m$, $c_{l\alpha} = 6.28$, $c_{m\beta} = -0.635$ and $x_\alpha = [0.0873 - (b+ab)]/b$.

The result for plunge and pitch motion are shown in fig. 9 and 10 for V = 15.2 m/s and a = -0.6. In fig 11 and 12 plunge and pitch motion are shown for V = 15.0 m/s and a = -0.4. For the open loop system a persistent periodic oscillations (limit cycles) in the pitch and plunge motion exists with velocity of 15.2 m/s, a = -0.6.
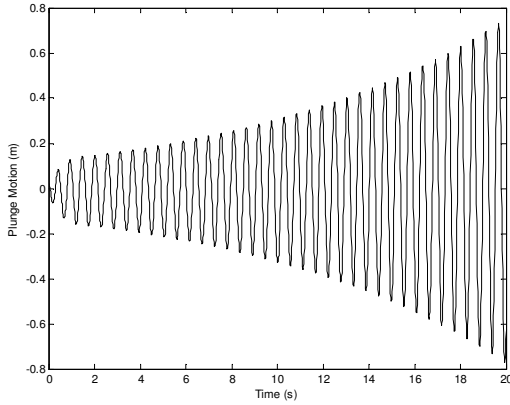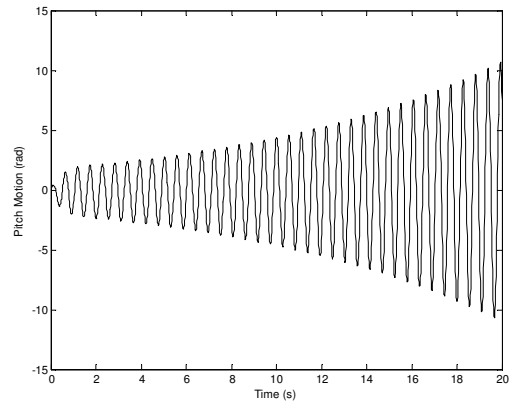

Figure 9: Plunge Motion for
V = 15.2 m/s and a = - 0.6

Figure 10 : Pitch Motion for
V = 15.2 m/s and a = - 0.6

5.2 CLOSED-LOOP SIMULATION

Control can be considered to be a manipulation to achieve or to fulfill a given objective. At this point a control law based in Quadratic Criterion Function (Meirovitch, 1998) is designed using Riccati equation method, for the linear controllable multivariable system

$$\dot{x} = Ax + Bu.......x(0) = x_0 \tag{11}$$

The controllability matrix for the system (7) is:

$$C = [B, AB, A^2 B, A^3 B] \tag{12}$$

and has rank 4 for all $x \in \Omega \subset R^4$. The controllability matrix is function of "U" and "a". The controllability matrix has been computed for several values of "U" and "a", the matrix C is nonsingular for $U \in [10, 30]$ and $\alpha \in [-0.6, 0.0]$, Fig. 13 and 14 shows the root locus of characteristic equation of (7) for U = 15.0 m/s and $a \in [-0.6, 0.0]/[0.0, 0.6]$. The performance of the closed loop system depends on the matrix A and the weighting matrices Q and R.

$$\beta = -R^{-1}B^T P x(t) \tag{13}$$
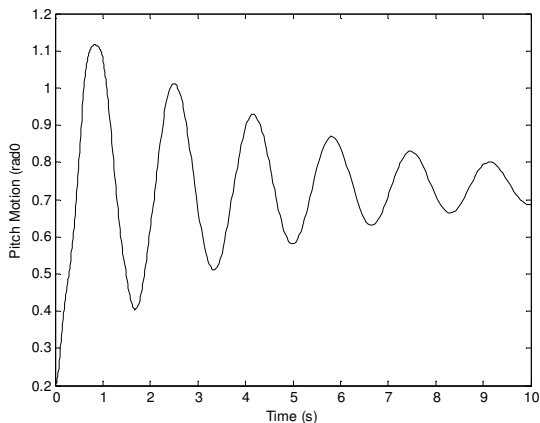
Figure 11: Pitch Motion for
V = 15.2 m/s and a = - 0.4
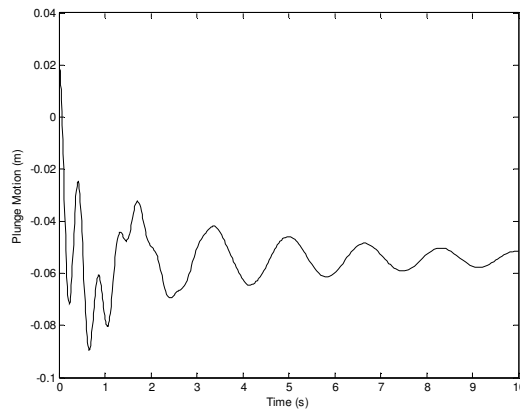
Figure 12: Plunge Motion for
V = 15.2 m/s and a = - 0.4

Substituting the control law (13) in (7) gives the closed loop system

$$\dot{x} = [A - BR^{-1}B^T P]x(t) = A_c x(t) \tag{14}$$
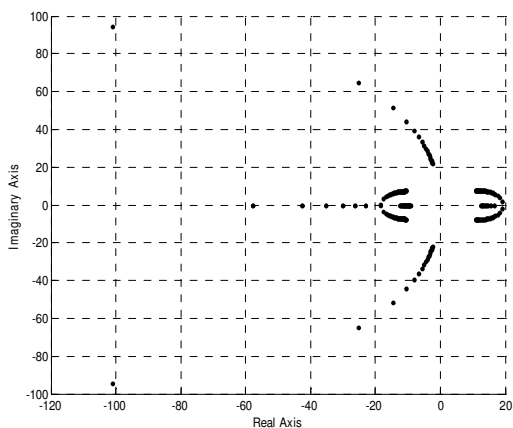
Figure 13. Root locus for
V = 15.0 m/s and $a \in [0.0, 0.6]$
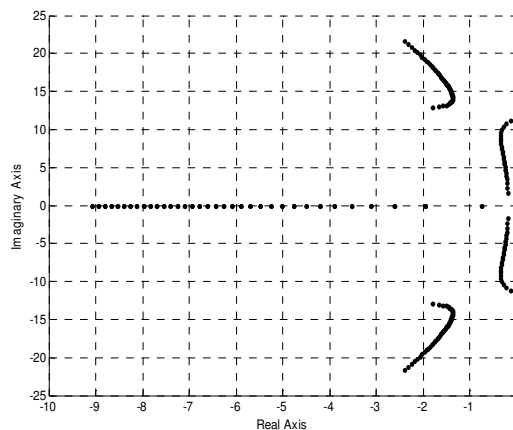
Figure 14. Root locus for
V = 15.0 m/s and $a \in [-0.6, 0.0]$

The matrix "C" has rank 4, for all $\in \Omega \subset R^4$, this implies that the system is completely state controllable. Using the parameters "U', "a", initial conditions, weighting matrix Q and R, respectively like in Singh (2002), Q = Diag(1,10,1,10) and R = 1000, respectively. The Eigenvalues of A_c are: -3.6859 ± 15.2378 i and -2.9777 ± 8.7803 i.
Using matrix P to calculate β in (13) and after some matrix manipulation we have the equations of motion as:

$$\begin{bmatrix} m & mx_\alpha b \\ mx_\alpha b & I_\alpha \end{bmatrix} \begin{Bmatrix} \ddot{h} \\ \ddot{\alpha} \end{Bmatrix} + \begin{bmatrix} c_h + \rho U b s_p c_{l\alpha} + c_1 & \rho U b^2 s_p c_{l\alpha}(1/2 - a) + c_2 \\ \rho U b^2 s_p c_{m\alpha} + c_3 & c_\alpha - \rho U b^3 s_p c_{m\alpha}(1/2 - a) + c_4 \end{bmatrix} \begin{Bmatrix} \dot{h} \\ \dot{\alpha} \end{Bmatrix} +$$

$$\begin{bmatrix} k_h + k_1 & \rho U^2 b s_p c_{l\alpha} + k_2 \\ 0 + k_3 & -\rho U^2 b^2 s_p c_{m\alpha} + k_4 \end{bmatrix} \begin{Bmatrix} h \\ \alpha \end{Bmatrix} = \begin{bmatrix} -\rho U^2 s_p b c_{l\alpha} \alpha_0 \\ \rho U^2 s_p b^2 c_{m\alpha} \alpha_0 \end{bmatrix} \tag{15}$$

where $c_1, c_2, c_3, c_4, k_1, k_2, k_3, k_4$ are function of $-BR^{-1}B^T P$.

Figures 15, 16 and 17 shows plunge, pitch and β motion, with velocity of 15.2 m/s and a = -0.4, Q = diag (1,10,1,10) and R = 1000, all the results were obtained using bond-graph modeling with 20-sim.

Figures 18, 19 and 20 shows plunge, pitch and β motion, with velocity of 15.2 m/s and a = -0.6, Q = diag (1,10,1,10) and R = 1000, all the results were obtained using bond-graph modeling with 20-sim.
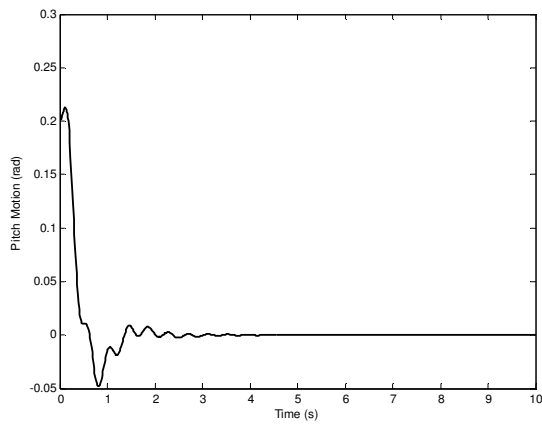

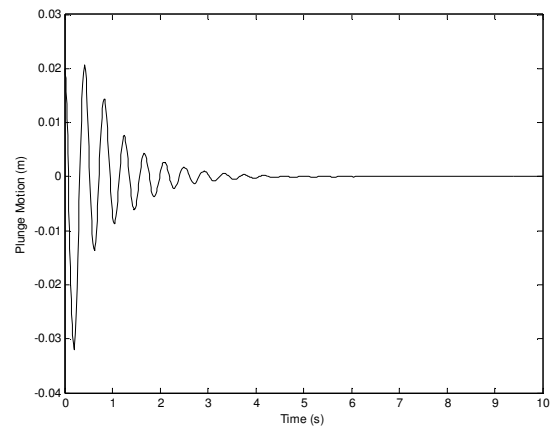Figure 15. Closed-loop Response for Pitch
Motion, V = 15.2 m/s and a = - 0.4

Figure 16. Closed-loop Response for Plunge
Motion, V = 15.2 m/s and a = - 0.4
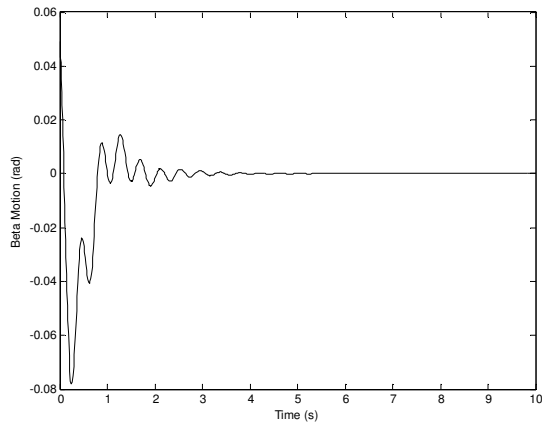
Figure 17. Closed-loop Response for Beta
Motion, V = 15.2 m/s and a = - 0.4
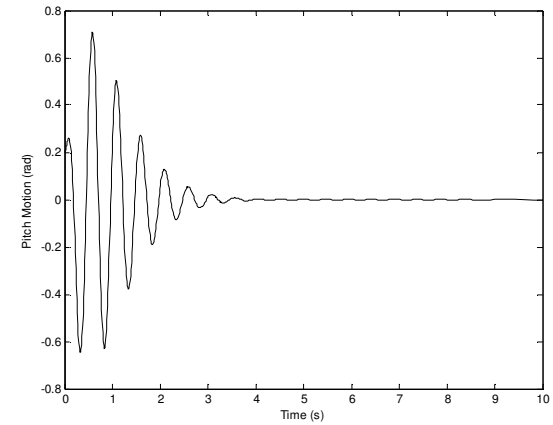
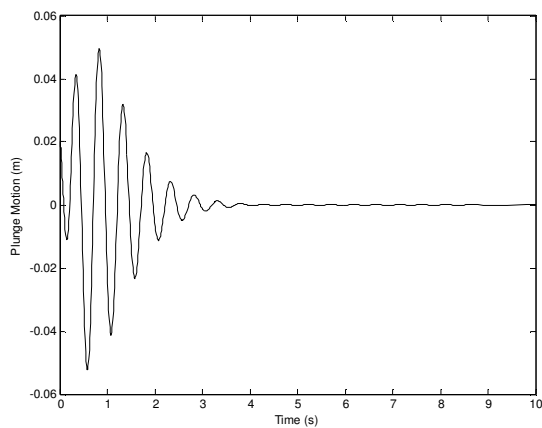Figure 18. Closed-loop Response for Pitch
Motion, V = 15.2 m/s and a = - 0.6

Figure 19. Closed-loop Response for Plunge
Motion, V = 15.2 m/s and a = - 0.6
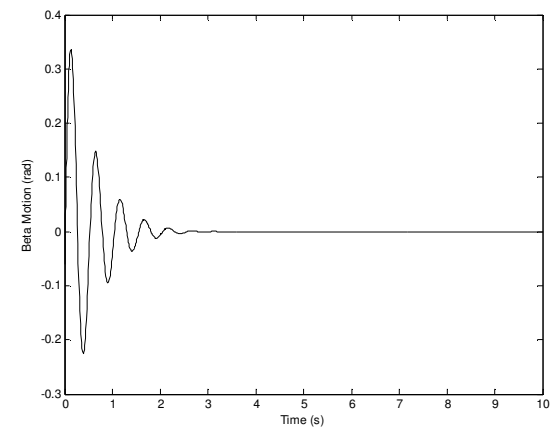

Figure 20. Closed-loop Response for Beta
Motion, V = 15.2 m/s and a = - 0.6

At last, two experiments were accomplished with speed of 30 m/s and different values for Q, diag(100,10,100,10) and diag(100,1000,100,1000). The results are presented in Figures 21, 22, 23, 24, 25 and 26.
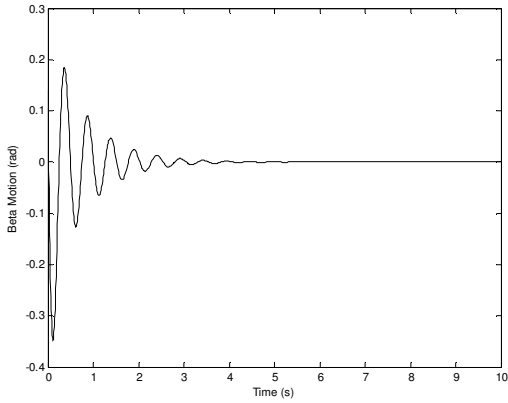
Figure 21. Closed-Loop Response for Beta
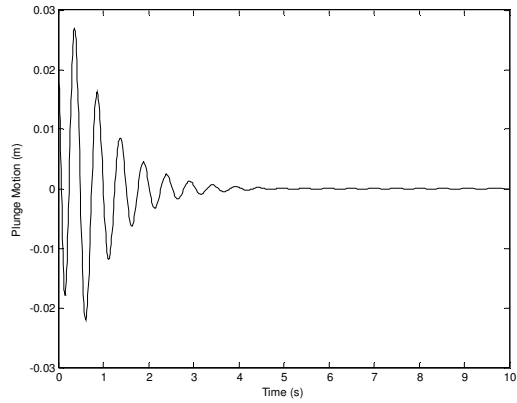Motion, V = 30 m/s and a = -0.6
Q = diag(100,10,100,10)

Figure 22. Closed-Loop Response for Plunge
Motion, V = 30 m/s and a = -0.6
Q = diag(100,10,100,10)

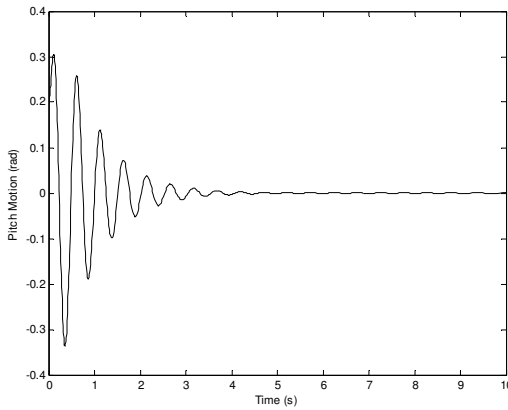
Figure 23. Closed-Loop Response for Pitch
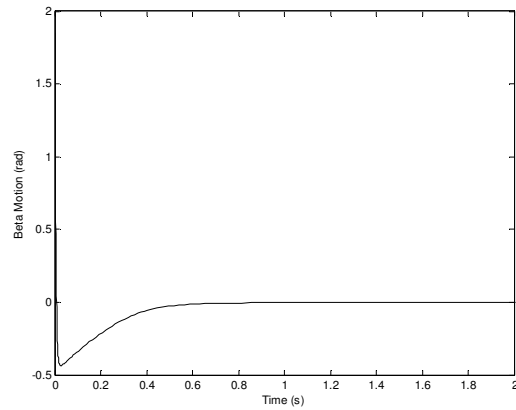Motion, V = 30 m/s and a = -0.6
Q = diag(100,10,100,10)

Figure 24. Closed-Loop Response for Beta
Motion, V = 30 m/s and a = -0.6
Q = diag(100,1000,100,1000)
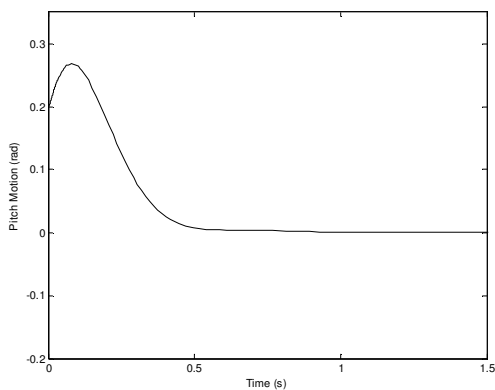

Figure 25. Closed-Loop Response for Pitch
Motion, V = 30 m/s and a = -0.6
Q = diag(100,1000,100,1000)
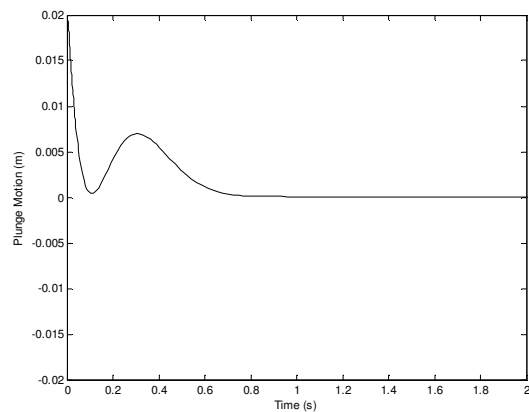
Figure 26. Closed-Loop Response for Plunge
Motion, V = 30 m/s and a = -0.6
Q = diag(100,1000,100,1000)

5. CONCLUSIONS

Herein, two aeroelastic dynamic models were considered, the first nonlinear using the theory of Theodorsen to express the forces and aerodynamic moments acting in a wing section with two degrees of freedom, plunge and pitch motion. In the second model the quasi-steady aerodynamic theory was considered to express the force and aerodynamic

moment. The two physical models were developed using the bond-graph modeling with 20sim. In the second model a single control surface was used for the flutter suppression.

The bond-graph model shows to be a powerful tool to simulate the aeroelastic system, the results are in good agreement with those reported in literature. It is possible to write models as directed graphs where parts are interconnected by bonds, along which exchange of energy occurs. The bond-graph modeling was shown quite effective for the analysis of the aeroelastic models developed.

By using the common rules and procedures, the bond-graph modeling diagram can be constructed for a certain dynamic system, and the interaction mechanism among the components can be determined, since the dynamic modeling is conducted directly in physical problem rather than the mathematical equations. This method is practical to use for multi-degree of freedom real wing structure, and due to the fact that simulation is executed directly in time domain, and the structural non-linear factors as function of dynamic response can be modeled accurately.

6. REFERENCES

Anderson, M., 1994, "Object-oriented modeling and simulation of hybrid systems", PhD Thesis, Lund Institute of Technology, Sweden;

Astrom K. J., Elmqvist, H., Mattson, S. E., 1998, "Evolution of continuous-time modeling and simulation", Proceedings of the 12th European Simulation Multiconference (ESM'98), SCS Publishing, Manchester UK, pp 9-18;

Bismarck M., 1997, "Structural Dynamics in Aeronautical Engineering", AIAA Education Series;

Block, J., Gilliart, H., 1997, "Active Control of an Aeroelastic Structure", AIAA, Aerospace Sciences Meeting & Exhibit, 35th, Reno, NV, Jan. 6-9, 1997;

Broenink J. F., 1999, "Introduction to Physical Systems Modeling with Bond Graphs", University of Twente, Dept EE, Control Laboratory PO Box 217, NL-7500 AE Enschede Netherlands;

Damic V., Cohodar M., "A Bond-Graph Approach to Modelling of Saptial Flexible Multibody Systems Based on Co-rotational Formulation, University of Sarajevo, Faculty of Mechanical Engineering, Bosnia and Herzegovina;

De Marchi C. J., Belo E. M., Marques F. D., 2005, "A Flutter Suppression Active Controles", Proceeding IMechE Vol. 219 Part G:J. Aerospace Engineering;

Emqvist, H., Cellier, F. E., and Otter, M., 1993, "Object Oriented modeling of hybrid systems", Proceding European Simulation Symposium, Delft, Netherlands, 31-41, 1993;

Fung, Y. C., 1955, "An Introduction to the Theory of Aeroelasticity", John Wiley and Sons, New York, 1955, pp. 207-215;

Karnopp D. C., Margolis D. L., Rosenberg R. C. 1990, "Systems Dynamics, a unified approach", 2nd edition, J Wiley, New York, 1990, NY, ISBN 0 471 45940 2;

Mattson, S. E., Elmqvist, H., and Broenink, J. F., 1997, "Modelica: An international effort to design the next generation modeling language", Journal A. Special Issue CACSD, vol 38 (3), pp 22-25;

Meirovitch L., 1990, "Dynamics and Control of Structures", John Wiley & Sons;

O'Neil, T., Strganac, T. W., 1998, "Aeroelastic Response of a rigid wing Supported by Nonlinear Springs", Journal of Aircraft, Vol. 35, N° 34, July-August 1998;

Pagwiwoko C. P., Said M. A. M., 2001, "A New method Development in Time Domain Simulation of Nonlinear Aeroelastic Vibrations", 4th Pacific International Conference on Aerospace Science and Techonology, Kaohsiung-Taiwan, 21-33 May 2001;

Paynter, H. M., 1961, "Analysis and design of engineering systems", MIT Press, Cambridge, MA;

Planitis G., Strganac T., 2004, "Control of a Nonlinear Wing Section Using Leading and Trailing Edge Surfaces", Journal of Guidance, Control, and Dynamics, Vol. 27, N° 1, January-February 2004;

Singh, S. N., Yim W., 2002, "State Feedback Control of an Aeroelastic System with Structural Nonlinearity", ELSEVIER, Aerospace Science and Technology, 2002;

Strganac, T. W., Ko, J., Thompson, D. E., "Identification and Control of Limit Cycle Oscillation in Aeroelastic Systems", Journal of Guidance, Control and Dynamics, Vol. 23, N° 6, November-December 2000;

Theodorsen, T. 1935, "General Theory of Aerodynamic Instability and Mechanism of Flutter", NACA Report 496;

Theodorsen, T., Garrick, I. E., 1940; "Mechanism of Flutter: A Theoretical and Experimental Investigation of the Flutter Problem", NACA Report 685.

7. RESPONSIBILITY NOTICE

The author(s) is (are) the only responsible for the printed material included in this paper.